

Mathematical Analysis for Prediction Performance Rate of Wheel Type Trenching Machine

Mohamed I. Ghonimy^{1,2}, Monier A. Morcos¹ and Abdalla E. Badr¹

¹Agricultural Engineering Dept., Faculty of Agriculture, Cairo University, Giza, Egypt.

² Department of Plant Production and Protection, College of Agriculture and Veterinary Medicine, Qassim University, Buraydah, Saudi Arabia.

Corresponding Author: Prof. Mohamed Ghonimy Email: mohamed.ghonimy@agr.cu.edu.eg, ORCID ID: <https://orcid.org/0000-0002-4887-3658>

ABSTRACT

The mathematical analysis for estimating the performance rate "*RP*" of wheel type trenching machine was studied. The mathematical analysis ended with an equation for this type. This mathematical equation was checked under different operating conditions. The practical study of the performance rate showed that the deviation of the theoretical performance rate from the actual performance rate ranged from five to seven percent for the 60.4 and 90.5 cm trench depth respectively. The machine field efficiency ranged between 43 and 50.1 percent for 90.5 cm and 60.4 cm trench depth respectively.

Keywords: Modeling, tile drainage, trencher performance.

INTRODUCTION

Drainage in agriculture means removing free water from soil in excess to its field capacity in the region of the root zone of the plants, in order to reach the best soil moisture-air balance that suits the growing crop. The functions of trenching machines are to mechanically perform the digging off the trenches, placing the tiles at the bottom of the trenches and back filling the soil in the trenches. There are mainly three types of trenching machines different in their construction and way of performance. These three types are chain type trenching machines, wheel type trenching machine and plow type trenching machines. Day (1973) defined the productivity of trenching machines as the rate the excavator can move along the trench line. He mentioned that the rate of excavation for a continuous trenching machine is its controlled productivity. It will vary

with the width and depth of trench, the toughness of the material to be excavated and the power available or selected by the operator. Peurifoy (1970) studied the productivity in trenching operations. He found many factors affecting the production rate of trenching machine. These include the class of soil, depth and width of trench, extent of shoring required, topography, climatic condition, extent of vegetation such as trees, stumps and roots, and physical obstruction, such as buried pipes, sidewalks, paved streets, building etc.

In case of laying a pipeline, the speed with which the pipe can be placed in the trench, also affect the production rate of the machine. Sitorus et al. (2016) reported that the digging machine forward speed, cutting depth, uniaxial compressive strength, and trench width are the most sensitive parameters affecting the power and angular speed. Design optimization using the information drawn from this parameter study can be preceded by focusing on the selection of traverse speed, uniaxial compressive strength, trench width, carrier weight, nose radius, bar length, and pivot point location. Spencer et al. (2007) described the principle features of the upgraded trencher and methods of calculating predicted trenching performance and they found that the target performance rate for wheel type trenching machine ranged from 80 to 400 m/h according to soil type. Schwap et al. (1966) studied the productivity in trenching operations. They found many factors affecting it such as; soil moisture, soil characteristics as hardness and stickiness, stones, and submerged stumps, depth of trench, conditions of the trenching machine, the skill of the operator, and the delays due to interruptions during operation. They found that an extremely wet soil may stop machine operation. Soil with a low moisture content may not affect the digging rate to any extent, but soil that stick to the buckets of the machine, sandy soils that fall apart easily, and deep cuts reduce digging speed. They also found that increasing the depth from 90 to 150 cm decreased the digging speed by 56 percent under Iowa and Minnesota conditions. Donahue et al. (1985) mentioned that the soil moisture, soil characteristics, skill of operator, width of the trench, and depth of the trench influence the factors affecting the capacity of the trenching machines. There is a several researches concerned with the use of mathematical models for trencher machines. Du, et al. (2016) found that the human operator control inputs to execute a work cycle of an excavator trenching operation. The simulation results in a work cycle that is generated by executing a series of tasks in the way a human operator would perceiving the state of the machine, deciding when to transition from one task to the next, and controlling the machine to

move the bucket through the tasks. The virtual operator model appropriately adapted to different operator control strategies, machine parameters changes (i.e. pump speed) and a change in work site goals (trench depth, pile location). The model-generated outputs based on human-like perception, decision-making, and action selection. Atangana Njock, et al. (2020) found that the success of jet trenching operations is closely related to some key factors including the soil conditions, trencher specifications, and characteristics of pipelines or cables. Three case histories are presented to demonstrate the importance of these key factors and their interrelationships. they also found that the performance of the jet trenchers on product burial is greatly dependent on the operation depth, soil conditions, the machine, and products specificities. When operating at a very large depth, most available models can achieve a maximum burial of 3 m within soils ranging from sand to stiff clays. The success of jet trenching operations also depends on the ability to accurately characterize the seabed sediments. Reddy and Shailesh (2018) mentioned that, in order to increase the life of backhoe excavator bucket tooth other two materials i.e. HSS and HCHCr has been analyzed for the similar force and boundary conditions. 3D model was prepared in solid works and software in FEM domain was utilized for analyzing the model or excavator bucket tooth behavior. Computational approach will give the results more close to practical values through simulation. Computer-Aided Engineering (CAE) can drastically reduce the costs associated with the product lifecycle. Whatever the type of the trenching machine is, it has the advantage of quite high rate of performance, since it simultaneously digs the trench, lays down the tiles or the pipes and, in some types, it also refills the ditches with the soil. This means fulfilling its complete function in a short period within the same day. It is characterized with the high accuracy in laying the pipes or the tiles at the required depth and slope. Besides, these types of trenching machines suppress the manual way of digging and laying drainage pipes by its lower costs of operation.

The purpose of this work was to find out the main factors affecting wheel type trenching machine performance rate, and to relate these affecting factors in mathematical relationships. These mathematical relationships was used to predict the performance rate of wheel type trenching machine.

MATERIAIS AND MTETHODS

Mathematical analysis approach

The wheel type trenching machine (Fig. 1) has its specific affecting mechanism which performs its required functions, the mathematical analysis had to be preceded with the

two main steps which were; to state the theory, the construction the specifications and the dimensions of the applied mechanism for wheel type trenching machine and to state the expected affecting factors on the performance of the applied mechanism, the nature and the magnitude of their effects. The performance rate of the trenching machine depends, to a great extent, on the forward speed of the machine. This forward speed in return, is related to both the size of the power source of the trenching machine and the magnitude of the consumed power during the performance of the machine. Therefore, the mathematical analysis depended on expressing the magnitude of any required power of the trenching machine as a function of machine forward speed. By equating the size of the power source with the summation of the required powers during machine performance (equation 1), the magnetite of the maximum machine forward speed can be estimated, and hence, the rate of performance of the machine can be determined.

$$P_b = P_c + P_r + P_i + P_s + P_t + P_e \pm P_a + P_n \quad (1)$$

Where:

P_b = brake power of the engine of the machine, kW;

P_c = pulling power needed for cutting, kW;

P_r = pulling power to overcome rolling resistance, kW;

P_i = pulling power to overcome slope resistance, kW;

P_s = power lost in slop resistance, kW;

P_t = power lost in transmission systems, kW;

P_e = power required to lift the cut soil, kW;

P_a = power required to overcome air resistance, kW;

P_n = power required to accelerate the machine to the operating speed due to its inertia, kW.

Both P_a and P_n could be neglected since the operating forward speeds of the trenching machine are very limited compared with any other moving truck. Therefore, equation (2) can be simplified as shown in the following equation (2).

$$P_b = P_c + P_r + P_i + P_s + P_t + P_e \quad (2)$$

The theory, construction, and specifications of the mechanisms of wheel type trenching machine:

The excavating unit of wheel type trenching machine, Fig. 2, consists of a rotating wheel equipped with buckets on its periphery. The cutting edge of the bucket may be

equipped with some teeth. The radius of the buckets cutting edges circular pathway from the wheel center to bucket cutting edges is (r). The wheel rotates at (n) rps. The depth of the digged trench is (d). The performance theory of wheel type trenching machine is that, while the machine moves horizontally at a speed (V_m), the wheel rotating speed (n) rps, and the cutting edges of the buckets move in curved paths almost following the ellipse equation (3). The cutting edges cut the soil in thin curved layers, and elevate it upwards. The direction and the speed of bucket cutting edge can be mathematically determined, with enough accuracy, using the ellipse equation.

To prove that, the pathway of the cutting edge of the bucket follows a curve close to that generated from the ellipse equation, Fig.3 shows the consecutive locations (X_i) and (Y_i) of bucket cutting edge. When bucket cutting edge just passes the vertical line through wheel center of rotation:

$$X_0 = 0 \quad Y_0 = r$$

At the consecutive different locations:

$$X_1 = r \sin \mu + V_m \cdot t \quad , \quad Y_1 = r \cos \mu$$

$$X_2 = r \sin 2\mu + V_m \cdot 2t \quad , \quad Y_2 = r \cos 2\mu$$

$$X_i = r \sin i\mu + V_m \cdot it \quad , \quad Y_i = r \cos i\mu$$

When bucket cutting edge just passes the horizontal line through wheel center of rotation:

$$X_{n^*} = r + V_m \times n^* t \quad , \quad Y_{n^*} = 0$$

Where:

n = Wheel rotating speed , rps

t . rev = Time of one revolution, $s^{-1} = 1/n$

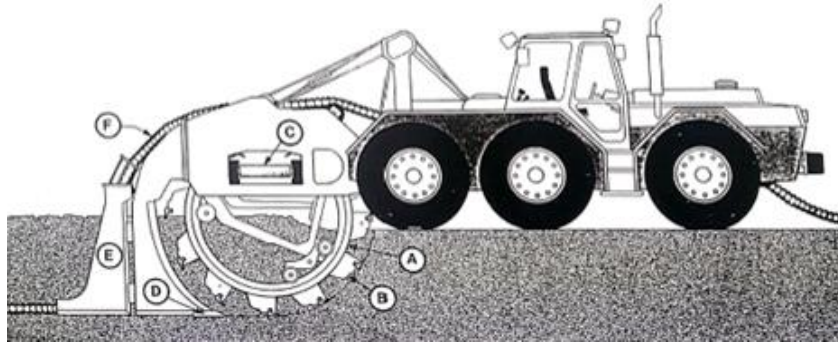
n^* = Number of divisions within an angle = $\pi/2 = 90^\circ$

μ = The central angle of each division = $\pi/2n^*$

t = Time needed for rotating an angle equal μ

$$t = \frac{1}{n} \times \frac{\mu}{2\pi} = \frac{1}{n} \times \frac{\pi}{2n^* \times 2\pi} = \frac{1}{4n \times n^*} \quad \text{sec}$$

$$n^* t = \frac{1}{4n} \quad \text{sec}$$



- A) Rotating wheel
 B) Digging buckets attached to wheel
 C) Cross conveyor for excavated earth
 D) Shoe to smooth trench bottom
 E) Tubing (tile) shute
 F) Corrugated drainage tubing

Fig. 1. Wheel type trenching machine.

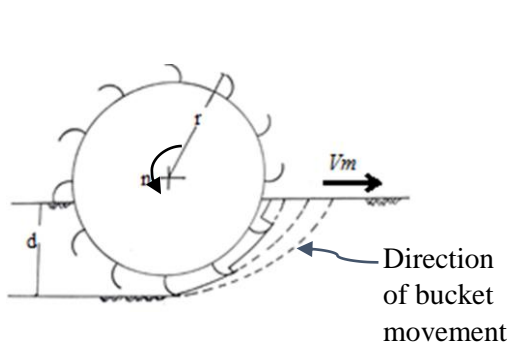


Fig. 2. The mechanism of wheel type trenching machine.

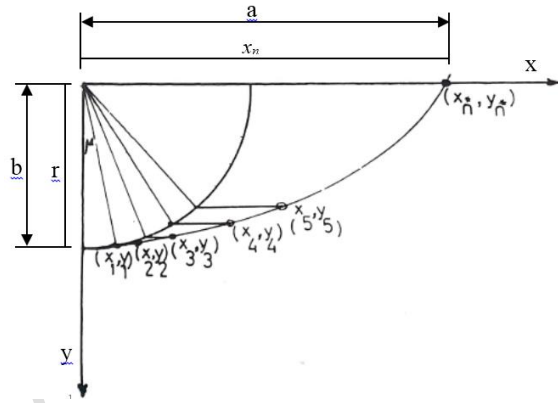


Fig. 3. The pathway of the bucket cutting edge for wheel type trenching machine.

If the ellipse equation applies to this case, equation (3), the values of (a) and (b) can be determined by substituting for

$$\frac{X^2}{a^2} + \frac{Y^2}{b^2} = 1 \quad (3)$$

X and Y for two cases, one when X = 0 and the other time when Y = 0

$$\text{When } X = 0 \quad b = r \quad (4)$$

$$\text{When } Y = 0 \quad a = r + V_m \cdot n^* t = r + V_m / 4n \quad (5)$$

and the general equation will be:

$$\frac{(r \cdot \sin i\mu + V_m \cdot it)^2}{(r + V_m \cdot n^* \cdot t)^2} + \frac{(r \cdot \cos i\mu)^2}{r^2} = 1 \quad (6)$$

To check this equation, the left side must be equal to 1 if the elliptic equation applies.

The left side of equation (6) can be written as:

$$\begin{aligned}
& \frac{r^2 \sin^2 i\mu + V_m^2 \cdot i^2 \cdot t^2 + 2r V_m \cdot i \cdot t \cdot \sin i\mu}{r^2 + V_m^2 \cdot n^{*2} \cdot t^2 + 2r \cdot V_m \cdot n^* \cdot t} + \cos^2 i\mu \\
&= \frac{r^2 \cdot \sin^2 i\mu + V_m^2 \cdot i^2 \cdot t^2 + 2r \cdot V_m \cdot i \cdot t \cdot \sin i\mu + r^2 \cos^2 i\mu + V_m^2 \cdot n^{*2} \cdot t^2 \cdot \cos^2 i\mu + 2r \cdot V_m \cdot n^* \cdot t \cdot \cos^2 i\mu}{r^2 + V_m^2 \cdot n^{*2} \cdot t^2 + 2r \cdot V_m \cdot n^* \cdot t} \\
&= \frac{r^2 (\sin^2 i\mu + \cos^2 i\mu) + V_m^2 \cdot n^{*2} \cdot t^2 \cdot \left[\left(\frac{i}{n^*} \right)^2 + \cos^2 i\mu \right] + 2r V_m \cdot n^* \cdot t \cdot \left(\frac{i}{n^*} \sin i\mu + \cos^2 i\mu \right)}{r^2 + V_m^2 \cdot n^{*2} \cdot t^2 + 2r \cdot V_m \cdot n^* \cdot t} \\
&= \frac{r^2 + V_m^2 \cdot n^{*2} \cdot t^2 \cdot \left[\left(\frac{i}{n^*} \right)^2 + \cos^2 i\mu \right] + 2r \cdot V_m \cdot n^* \cdot t \cdot \left(\frac{i}{n^*} \cdot \sin i\mu + \cos^2 i\mu \right)}{r^2 + V_m^2 \cdot n^{*2} \cdot t^2 + 2r \cdot V_m \cdot n^* \cdot t} \quad (7)
\end{aligned}$$

The values of the left side of equation (6) equal 1 when $i=0$ and the angle $(i\mu) = 0$ or when $i = n^*$ and $i\mu = \pi/2$, but it deviates in between. The deviation is very small and can be ignored since both the value of $(V_m^2 \cdot n^{*2} \cdot t^2)$ and $(2r \cdot V_m \cdot n^* \cdot t)$ are very small compared with the value of (r^2) . When reasonable values of the parameters in the left side of equation (6) was considered. The deviation was computed for different values of $(i\mu)$ as shown in table (1).

Table 1- The deviation of the actual pathway of bucket cutting edge from the curve of the equation of ellipse.

$i\mu$	0	$\pi/12$	$\pi/6$	$\pi/4$	$\pi/3$	$\pi/2.4$	$\pi/2$
Deviation, %	0	-0.37	-1.2	-2.3	-1.93	-1.69	0

Thus, the computed deviations were less than -2.3 Percent.

Factors affecting the performance of the trenching machine

There are many factors affecting the performance rate of the trenching machine. These factors can be classified into two groups; **soil factors** which include; soil specific weight (ω), N.cm^{-3} , soil unit draft (U), N.cm^{-2} , traction coefficient, rolling resistance coefficient (RR), angle between inclined soil surface and the horizontal direction (ψ), and friction coefficients between soil and soil and between soil and metal (F_{ms}).

Machine factors which include; machine weight (W_m), N, machine brake power (P_b), kW, machine forward speed (V_m), m s^{-1} , trench cutting width (W_t), cm, vertical depth of the cut trench (d), cm, slip percentage of the tractor device of the machine (S), machine transmission efficiency (η_t), machine field efficiency (η_f), wheel radius (r), m, wheel rotating speed (n), rps, and the number of buckets on the wheel (N_B).

Some assumptions and simplifications were done in order to facilitate mathematical manipulation. These include Homogeneous and isotropic soil, with a constant unit draft. Constant velocities for any moving element, i.e., constant machine forward speed, and

constant rotating for the rotating wheel were assumed. The path of the cutting edge was considered elliptical in shape.

Mathematical analysis steps

The mathematical analysis for estimating the performance rate (RP) of the wheel type trenching machine is expected to be in the form of the equation (8):

$$RP = 60 \times V_m \times \eta_t \quad (8)$$

Where:

RP = the actual performance rate of the machine, $m \text{ min}^{-1}$;

V_m = the machine forward speed, $m \text{ s}^{-1}$;

η_f = the field efficiency.

To find out the value of V_m , the components of equation (2*) were obtained as the following:

$$P_c + P_r + P_i + P_s + P_t + P_e - P_b = 0 \quad (2^*)$$

a) Determination of P_c

Referring to fig. 4, the pulling power needed for cutting depends on the cutting force (F_c) and the absolute speed of the bucket cutting edge (V_{bi})

$$P_c = 0.001 \left(\sum_{i=1}^N F_{ci} \cdot V_{bi} \right)$$

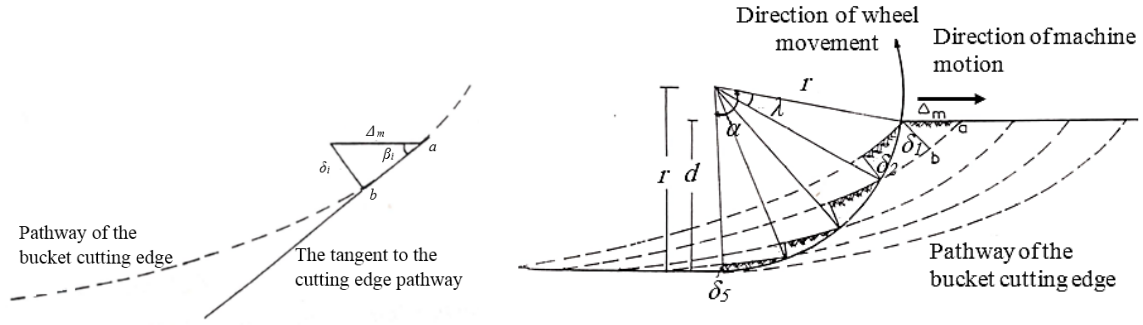
$$P_c = 0.001 K^* \cdot U \cdot W_t \cdot \sum_{i=1}^N V_{bi} \cdot \delta_i \quad kW$$

Referring to fig. (4),

$$N = \frac{\alpha}{\lambda} = \frac{\cos^{-1} \left(1 - \frac{d}{100r} \right)}{2\pi/N_B}$$

Where V_{bi} is the absolute speed of bucket i ; δ_i is the cut layer thickness of bucket i ; N_B is the number of buckets for the wheel and N is the number of bucket cutting the soil simultaneously.

$$\delta_i = \frac{100 V_m}{n \cdot N_B} \cdot \sin \beta_i \quad (9)$$



The difference in cut layer thickness on the pathway of bucket cutting edge.

Fig. 4. Determination the thickness of the cut layer for wheel type trenching machine.

The angle β_i is the angle between the horizontal direction and the tangent to the curve representing bucket (i) cutting edge pathway and it can be obtained from differentiating ellipse equation;

$$\beta_i = \tan^{-1} \left[\frac{b}{a} \cdot \left(\frac{a^2}{x_i^2} - 1 \right)^{-1/2} \right]$$

Where:

$$b = r, \quad a = r + (V_m/4n), \quad (x_i)^2 = a^2 [1 - (y^2/b^2)], \quad \text{and } y_i = r \cdot \cos [\alpha - (i - 1) \cdot \lambda]$$

$$\beta_i = \tan^{-1} \left[\left(\frac{1}{1 + (V_m/4r \cdot n)} \right) \cdot \tan(\alpha - (i - 1) \cdot \lambda) \right]$$

$$\beta_{max} = \tan^{-1} \left[\left(\frac{1}{1 + (V_m/4r \cdot n)} \right) \cdot \tan \alpha \right] \quad (10)$$

Using reasonable values for the parameters for the determination of $\sum_{i=1}^N \delta_i$ showed that its value = $2.31 \delta_{max}$ with only a deviation of $\pm 1.5\%$. Also, instead of using V_{bi} , it was found that using the average speed V_b did not give any serious error.

From the ellipse equation,

$$\bar{V}_b = \pi \cdot n \cdot (2r + (V_m/4n)) \quad (11)$$

So,

$$P_c = 0.001 \times \frac{231\pi \cdot K^* \cdot U \cdot W_t \cdot V_m}{N_B} \cdot [2r + (V_m/4n)] \cdot \sin \beta_{max} \quad (12)$$

b) Determination of P_r

$$P_r = 0.001 F_r \cdot V_m, \quad (\text{Ranjbarian et al., 2017})$$

The resistance force (F_r) due to rolling resistance depends on machine weight (W_m), the weight of cut soil (W_s), the rolling resistance coefficient (RR), the vertical component of

the cutting force (F_{cv}), and the angle ψ between inclined soil surface and the horizontal direction.

$$P_r = 0.001 V_m \cdot RR \cdot (W_m + W_s + F_{cv}) \cdot \cos\psi$$

Referring to Figs (5) and (6), the complete volume of cut of one bucket b_v

$$b_v = \frac{100 d \cdot W_t \cdot V_m}{n \cdot N_B}$$

While the incomplete volumes of cut of the other buckets could be considered proportional as the areas of the triangles with the same base Δm and decreasing heights L_i with,

$$\sum_{i=1}^N L_i = \sum_{i=1}^N L_i \left(\frac{N - (i - 1)}{N} \right)$$

Also, the weight of soil would include the cut soil in other buckets to the top of the rotating wheel. so, the total volume of cut soil b_{VT} could be

$$b_{VT} = \frac{W_t \cdot \Delta m \cdot L_i}{2} \cdot \left[\frac{1}{N} (N + (N - 1) + (N - 2) + \dots + 1) + \left(\frac{N_B}{2} - N \right) \right]$$

$$b_{VT} = \frac{W_t \cdot \Delta m \cdot L_i}{2 \times 2} \cdot (1 + N_B - N)$$

$$W_s = \frac{100 d \cdot W_t \cdot V_m \cdot \omega}{2 \cdot n \cdot N_B} \cdot (1 + N_B - N)$$

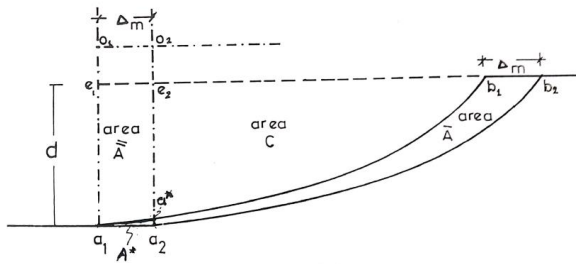
Referring to fig. 7, the vertical component F_{cv} of the cutting force F_{ci} would be $F_{ci} \cdot \sin\beta$.

So, the summation of the vertical component of the cutting force would be:

$$F_{cv} = \frac{100 K^* \cdot U \cdot W_t \cdot V_m}{n \cdot N_B} \cdot \sum_{i=1}^N \sin\beta_i \cdot \sin\beta_i$$

Using reasonable values for the parameters for the determination of $\sum_{i=1}^N \sin^2\beta_i$ should that its value = $1.77 \sin^2\beta_{max}$ with only a deviation of $\pm 1.25\%$. So,

$$P_r = 0.001 RR \cdot V_m \cdot \cos\psi \cdot \left(W_m + \frac{100 d \cdot W_t \cdot V_m \cdot \omega}{2 \cdot n \cdot N_B} \cdot (1 + N_B - N) + \frac{177 K^* \cdot U \cdot W_t \cdot V_m}{n \cdot N_B} \cdot \sin^2\beta_{max} \right) \quad (13)$$



$$A = A^* + A' = A^* + A''$$

$$\Delta_m = 100V_m \cdot \frac{1}{n \cdot N_B}$$

Fig. 5. Determination the area (A) between the pathway curves of two consecutive bucket cutting edges.

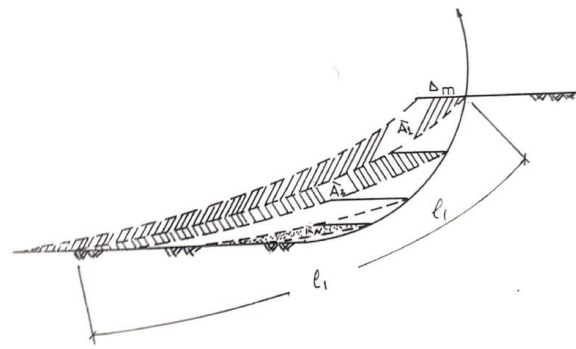


Fig. 6. The determination of the volume of the cut elevated soil.

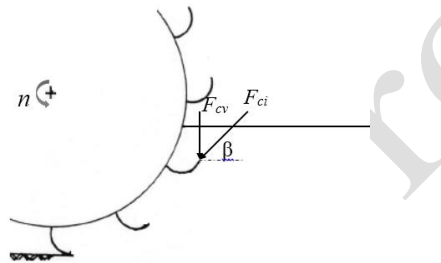


Fig. 7. Cutting force (F_{ci}), vertical component of cutting force F_{cv} and angle β between the horizontal direction and the tangent to the curve representing bucket "i" cutting edge pathway.

c) Determination of P_i

The pulling power to overcome slope resistance (P_i) depends on the weight of the machine (W_m), the weight of cut elevated soil (M_s), the machine forward speed (V_m), and the angle (ψ) between the inclined soil surface and the horizontal direction.

$$P_i = 0.001 V_m \cdot \sin\psi \cdot [W_m + W_s]$$

$$P_i = 0.001 V_m \cdot \sin\psi \cdot \left[W_m + \frac{100 d \cdot W_t \cdot V_m \cdot \omega}{2 \cdot n \cdot N_B} \cdot (1 + N_B - N) \right] \quad (14)$$

d) Determination of P_s

$$P_s = 0.001(F_c + F_r) \cdot \left(\frac{s}{100-s} \right) \cdot V_m \quad (\text{Ranjbarian et al., 2017})$$

$$P_s = 0.001 \left\{ \frac{231K^* \cdot U \cdot W_t \cdot V_m}{n \cdot N_B} \cdot \sin \beta_{max} + RR \cdot \cos \psi \cdot \left[W_m + \frac{100 d \cdot W_t \cdot V_m \cdot \omega}{2 \cdot n \cdot N_B} \cdot (1 + N_B - N) + \frac{177 K^* \cdot U \cdot W_t \cdot V_m}{n \cdot N_B} \cdot \sin^2 \beta_{max} \right] \right\} \cdot \left(\frac{S}{100 - S} \right) \cdot V_m \quad (15)$$

e) Determination of P_t

$$P_t = P_b \cdot (1 - \eta_t) \quad (16)$$

f) Determination of P_e

Referring to Fig. (8), the power P_e required to lift the cut soil would be:

$$P_e = 0.001 \frac{W_r}{t_{rev}} = 0.001 \times \frac{10^2 \cdot \omega \cdot b_{v1} \cdot N_B \cdot \left(2r - \frac{2d}{300} \right)}{t_{rev}}$$

$$P_e = 0.1 \times \omega \cdot W_t \cdot d \cdot V_m \cdot \left(2r - \frac{2d}{300} \right) \quad (17)$$

Referring to equations (2*), (12), (13), (14), (15), (16) and (17);

$$\begin{aligned} V_m^2 [10^4 RR \cdot \cos \psi \cdot \omega \cdot W_t \cdot d \cdot (1 + N_B - N) + (3.54 \times 10^4 RR \cdot \cos \psi \cdot K^* \cdot U \cdot W_t \cdot \sin^2 \beta_{max}) \\ + (462 K^* \cdot U \cdot W_t \cdot (25\pi + S(1 - \pi/4)) \cdot \sin \beta_{max}) \\ + (10^2 \times \omega \cdot W_t \cdot d \cdot (1 + N_B - N) \cdot \sin \psi)] \\ + V_m \left[200n \cdot N_B \cdot RR \cdot \cos \psi \cdot W_t + (2n \cdot N_B \cdot W_m \cdot (100 - S) \cdot \sin \psi) \right. \\ \left. + (924\pi \cdot K^* \cdot U \cdot W_t \cdot r \cdot n \cdot (100 - S) \cdot \sin \beta_{max}) \right. \\ \left. + \left(2 \times 10^2 n \cdot N_B \cdot (100 - S) \cdot \omega \cdot W_t \cdot d \cdot \left(2r - \frac{2d}{300} \right) \right) \right] \\ - (2000P_b \cdot \eta_t \cdot N_B \cdot (100 - S)) = 0 \quad (18) \end{aligned}$$

$$V_m^2 + \frac{G}{Q} \cdot V_m - \frac{J}{Q} = 0 \quad (19)$$

Where:

$$Q = Q_1 + Q_2 + Q_3 \quad (19a)$$

$$G = G_1 + G_2 + G_3 \quad (19b)$$

$$G_1 = n \cdot N_B \cdot W_m \cdot (100RR \cdot \cos \psi - (100 - S) \cdot \sin \psi) \quad (19c)$$

$$G_2 = 924\pi \cdot K^* \cdot U \cdot W_t \cdot r \cdot n \cdot (100 - S) \cdot \sin \beta_{max} \quad (18d)$$

$$G_3 = 2 \times 10^2 n \cdot N_B \cdot (100 - S) \cdot \omega \cdot W_t \cdot d \cdot \left(2r - \frac{2d}{300} \right) \quad (19e)$$

$$Q_1 = 10^2 \times \omega \cdot W_t \cdot d \cdot (1 + N_B - N) \cdot [100RR \cdot \cos \psi + \sin \psi] \quad (19f)$$

$$Q_2 = 462 K^* \cdot U \cdot W_t \cdot (25\pi + S(1 - \pi/4)) \cdot \sin \beta_{max} \quad (19g)$$

$$Q_3 = 3.54 \times 10^4 RR \cdot \cos\psi \cdot K^* \cdot U \cdot W_t \cdot \sin^2 \beta_{max} \quad (19h)$$

$$J = 2000 P_b \cdot \eta_t \cdot N_B \cdot (100 - S) \quad (19i)$$

Applying the rule:

$$V_m = -\frac{b}{2} \pm \sqrt{\left(\frac{b}{2}\right)^2 - \frac{c}{a}} \quad (20)$$

$$\frac{b}{2} = \frac{G}{2Q} \quad (20a) \quad \text{and} \quad C = \frac{J}{Q} \quad (20b)$$

Equation (20) can be solved for V_m by trial and error method, by giving a reasonable initial values for V_m to solve equations (20a) and (20b). Using reasonable values for the parameters of equation (20) and using different values of K^* ranged from 1 to 15, resulted in V_m value ranging from 1.38 to 0.17 m sec⁻¹.

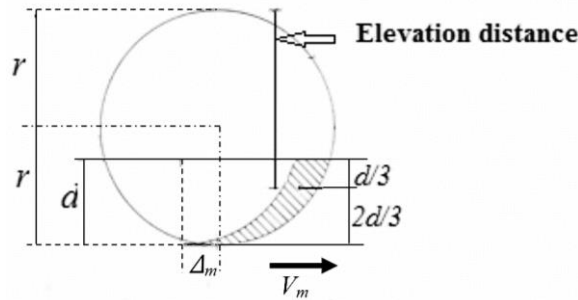


Fig. 8. The elevation distance of the cut soil in wheel type trenching machine.

The actual performance rate (RP) could be obtained from equation (8) using field efficiency $\eta_t = \eta_s \cdot \eta_w \cdot \eta_{ti}$, where η_s is the efficiency of utilizing the geared speed, η_w is the efficiency of utilizing the proposed width of the machine, and η_{ti} is the efficiency of utilizing the time. However, due to the very low speed of the machine and the actual & theoretical machine width during operation was equals, both η_s and η_w could be considered equal to 1.0.

Field experimental work

The experimental work was carried out through a period of almost one year. The area was in Dakahlia Governorate, meet Ghmr center, Shalaby wa el-Serw village (intersection of latitude 30.7167 and longitude 31.2525), in which the wheel type trenching machine was tested. The specifications of the machine is shown in table (2). Trench depths of 60 and 90 cm were tested.

Table 2- Technical specifications of the wheel type trenching machine.

Engine	Daimler Benz (Mercedes) Diesel
Power	130 kW (178 HP) at 1750 rpm
Tank capacity	Fuel 306 lit., Oil 120 lit.
Electricity	24 V1
Transport speed	0 - 5.0 km h ⁻¹
Ground pressure	approx. 3.1 N cm ⁻²
Transmission efficiency	90 %
<u>Digging unit</u>	
Rotating wheel speed	1 st speed: 8 rpm. 2 nd speed: 19 rpm. 3 rd speed: 26 rpm. 4 th speed: 34 rpm. 5 th speed: 45 rpm. Reverse: 6 rpm.
Wheel diameter	2400 mm.
Buckets number	16
Max. trench depth	1100 mm.
Trench width	350 - 560 mm.
<u>Transport data</u>	
length	8750 mm
Width	8000 mm
Height	2720 mm
Weight	11.562 tons

RESULTS AND DISCUSSION

The average rolling resistance coefficient of the experimental field was taken as 4.0 percent, since it was found ranging between 3.0 and 5.0 percent (Jia and Jia, 2018). The average specific weight of the soil (ω) was found to be 0.011 N cm⁻³ (Jia and Jia, 2018). In addition, the average draft was taken as 10 N cm⁻² (Jia and Jia, 2018). The average values of field measurements were as shown in Table (3).

Table 3- Average values of field measurements.

Field measurements	Ave.	SD	Ave.	SD
Trench depth, cm	60.4	3.1	90.5	3.8
Trench width, cm	35.1	1.15	35.1	1.15
Slip percentage, %	5	---	7	---
Machine forward speed, m s ⁻¹	0.33	0.02	0.28	0.11
Wheel rotating speed, rps	0.43	---	0.32	---
K^* ; A dimensionless coefficient	12	---	12	---
Angle between inclined soil surface and the horizontal direction, degree	0	---	0	---

Actual performance rate (RP) and field efficiency (η_f)

Table (4) show the breakdown items of the daily machine time, as practically measured in the field. They also show the average of the actual performance rate of the machine and its efficiency.

Table 4- Breakdown items of the daily machine item for the used wheel type trenching machine and its average performance rate and field efficiency.

Activities	*Average spent time, min day ⁻¹		SD, min day ⁻¹	
	Trench depth, cm		Trench depth, cm	
	60.4	90.5	60.4	90.5
Net excavating and pipe laydown	213	180	4.23	5.31
Turning and travelling to start digging another trench	63	71	2.18	2.79
Setup time for reaching the depth	21	33	1.94	2.15
Rest periods	60	60	2.14	2.19
Field quick maintenances	24	27	1.14	2.20
Refill of water and oil tank	23	30	2.23	1.97
Other lost time	21	18	2.19	3.19
Average total time, min day ⁻¹	425	419	1.49	5.01
**Total installed length, m day ⁻¹	3760	2677	3.15	4.22
Actual performance rate, m min ⁻¹	8.85	6.39	2.19	1.23
*** Field efficiency, %	50.1	43.0	2.16	1.18

Theoretical deterioration of the wheel type trenching machine performance rate

To theoretically predict the performance rate of the wheel type trenching machine, equations (8), (20), (20a), and (20b) were used. The specifications of the applied wheel type trenching machine is shown in tales (2). In addition, the field-measured data are shown in table (3). Using the above mentioned data into equation (20a) for the value of $b/2$ and into equation (20b) for the value of C gave the following equations:

1. For 60.4 cm depth

$$\frac{b}{2} = \frac{1}{2} \times \frac{13873002.47 + 599354145.38 \sin\beta_{max}}{111938.11 + 154922100.1 \sin\beta_{max} + 5964192 \sin^2\beta_{max}}$$

$$C = \frac{172060200}{111938.11 + 154922100.1 \sin\beta_{max} + 5964192 \sin^2\beta_{max}}$$

Where:

$$\beta_{max} = \tan^{-1} \frac{1}{1 + \frac{V_m}{2.064}}$$

Solving equation (20) by trial and error method, gave the computed values of (V_m), Table (5). Applying the computed value of (V_m) into equation (8), gave the predicted value of the performance rate of the wheel type trenching machine:

$$RP = 60 \times 0.309 \times 0.501 = 9.29 \text{ m min}^{-1}.$$

This predicted value was very close to the experimentally determined value of the performance rate for the 60.4 cm trench depth, which was found to be 8.85 m min⁻¹, Table (5) and Fig. (9). The deviation of the theoretically computed value from the field determined value for the performance rate was only about 5.0 percent.

2. For 90.5 cm depth

$$\frac{b}{2} = \frac{1}{2} \times \frac{1195399.9 + 436640065.7 \sin \beta_{max}}{223629.12 + 155757306.5 \sin \beta_{max} + 5964192 \sin^2 \beta_{max}}$$

$$C = \frac{125349120}{223629.12 + 155757306.5 \sin \beta_{max} + 5964192 \sin^2 \beta_{max}}$$

Where:

$$\beta_{max} = \tan^{-1} \frac{3.9288}{1 + \frac{V_m}{1.536}}$$

Solving equation (20) by trial and error method, gave the computed values of (V_m), Table (5). Applying the computed value of (V_m) into equation (8), gave the predicted value of the performance rate of the wheel type trenching machine:

$$RP = 60 \times 0.265 \times 0.43 = 6.84 \text{ m min}^{-1}$$

This computed value was very close to the experimentally determined value of the performance rate for the 90.5 cm trench depth, which was found to be 6.39 m min⁻¹, Table (5) and Fig. (9). The deviation of the theoretically computed value from the field determined value for the performance rate was only about +7.0 percent.

Table 5- The initially proposed and the computed values in the interaction process for the determination of the forward speed of the wheel type trenching machine at 60.4 cm and 90.5 cm depths. (Using trial and error method)

60.4 cm trench depth	V_m proposed value, m s ⁻¹	3	1	0.4	0.309
	V_m computed value, m s ⁻¹	0.429	0.336	0.310	0.309
90.5 cm trench depth	V_m proposed value, m s ⁻¹	3	1	0.4	0.265
	V_m computed value, m s ⁻¹	0.312	0.276	0.267	0.265

The findings of the used wheel type trenching machine show the degree of accuracy of the mathematically derived equations. These derived equations can be used with enough

confidence to theoretically predict the performance rate of wheel type trenching machine depending on the prevailing operating conditions.

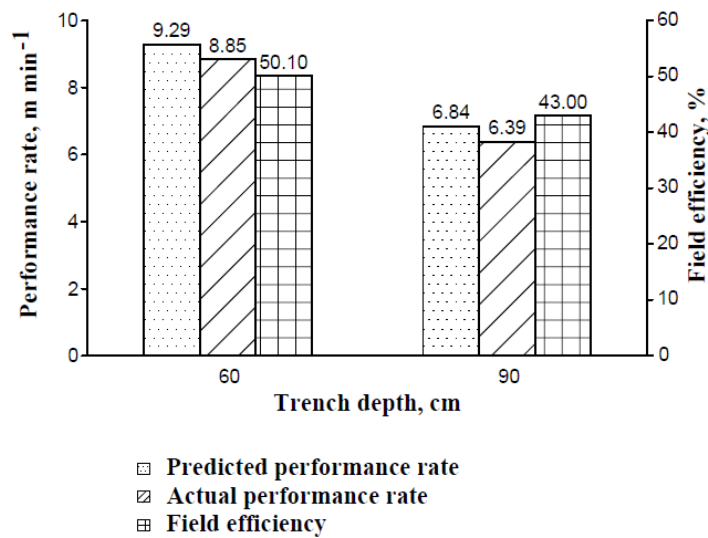


Fig. 9. The actual & predicted performance rate and field efficiency of the wheel type trenching machine.

CONCLUSION

The digging of the trenches is an important process in order to implement the tail drainage projects. This research is concerned with studying the relationship that correlate the performance of the wheel type trencher machine with the factors affecting them, so that the rate of performance can be predicted or controlled through the factors affecting it. Also, a field operating study was conducted under actual operating conditions to test the validity of the derived mathematical equations.

The study showed the validity of the derived equations in predicting the performance rate of chutes. The percentage difference between the performance rate calculated from the equations and the actual field estimated performance rate were 5 and 7% for cutting wheel when they worked at a trench depth of 60.4 and 90.5 cm, respectively. Also, the field efficiency were 43 and 50.1% when the machine working at a trench depth of 60.4 and 90.5 cm, respectively.

REFERENCES

- Atangana Njock, P. G., Q Zheng, N. Zhang, and Y. S. Xu. 2020. Perspective Review on Subsea Jet Trenching Technology and Modeling. *Journal of Marine Science and Engineering*, 8(6), 460. <https://doi.org/10.3390/jmse8060460>
- Day, D.A. 1973. *Construction equipment guide*. John Wiley and Sons.,Inc., N. Y., USA, 206-208.

- Donahue, R.L., R.W. Miller, and G.C. Shickluna. 1985. Soil an introduction to soil and plant growth. 4th Ed. Prentice Hall, Inc., Englewood cliffs, Newjersey, USA. 98-106.
- Du, Y., M. C. Dorneich, and B. Steward. 2016. Virtual operator modeling method for excavator trenching. *Automation in construction*, 70, 14-25.
DOI: [10.1016/j.autcon.2016.06.013](https://doi.org/10.1016/j.autcon.2016.06.013)
- Jia, J., and Jia. 2018. *Soil dynamics and foundation modeling*. New York: Springer.
- Peurifoy, R.L. 1970. *Construction planning, equipment, and methods*. 2nd ed. McGraw, Hill Kogakusha, Ltd., Tokyo, Japan, pp 695.
- Ranjbarian, S., M. Askari, and J. Jannatkah. 2017. Performance of tractor and tillage implements in clay soil. *Journal of the Saudi Society of Agricultural Sciences*, 16(2), 154-162. <https://doi.org/10.1016/j.jssas.2015.05.003>
- Reddy, Y., and P. Shailesh. 2018. Design and Analysis of Excavator Bucket Tooth. *International Journal of Modern Trends in Engineering and Research*, 5(4), 79-86.
DOI:10.21884/IJMTER.2018.5106.Q4FBI.
- Schwab, G.O., R.K. Frevert, T.W. Edminster, and K.K.Barnes. 1966. *Soil and water conservation engineering*. 3rd Ed. 214-218.
- Sitorus, P.E., J.H. Ko, and O.S. Kwon. 2016. Parameter study of chain trenching machines of Underwater Construction Robots via analytical model. In *OCEANS 2016 MTS/IEEE Monterey* (pp. 1-6). IEEE. DOI: [10.1109/OCEANS.2016.7761072](https://doi.org/10.1109/OCEANS.2016.7761072)
- Spencer, A., J. Machin, and E. Jackson. 2007. Rock cutting With the T750 super trencher. *Unmanned Intervention*, New Orleans, LA, 30.